# *n*-Type Organic Field-Effect Transistors with High Electron Mobilities Based on Thiazole−Thiazolothiazole Conjugated Molecules

Masashi Mamada,[†] Jun-ichi Nishida,[†] Daisuke Kumaki,[‡] Shizuo Tokito,[‡] and Yoshiro Yamashita*,[†]

*Department of Electronic Chemistry, Interdisciplinary Graduate School of Science and Engineering, Tokyo Institute of Technology, Nagatsuta, Midori-ku, Yokohama 226-8502, Japan, and NHK Science and Technical Research Laboratories, Kinuta, Setagaya-ku, Tokyo 157-8510, Japan*

*Received June 5, 2007. Revised Manuscript Received August 16, 2007*

Two novel thiazolothiazole derivatives with trifluoromethylphenyl groups were synthesized and characterized by differential scanning calorimetry, X-ray single crystal analysis, UV−vis absorption spectroscopy, cyclic voltammetry, field-effect transistor (FET) characteristics, and X-ray diffraction. The FET characteristics of thiazole−thiazolothiazole derivatives are strongly dependent on the nitrogen positions. The derivative with a 2-(4-trifluoromethylphenyl)thiazole unit afforded a high performance FET device that showed a high electron mobility of 0.12 $cm^2\ V^{-1}\ s^{-1}$ with a bottom contact configuration. Moreover, with a top contact configuration, high electron mobilities of 0.24−0.64 $cm^2\ V^{-1}\ s^{-1}$ and low threshold voltages of 18−24 V depending on the surface modification were achieved. The relationship between molecular structure, molecular packing, electrical characteristics, film structure, and FET performance were investigated.

## Introduction

Organic field-effect transistors (OFETs) are of great interest in applications such as display drivers, identification tags, and smart cards because they have the advantages of being inexpensive, flexible, and lightweight.[1] Since the report of the first OFET in 1986,[2] there has been great progress in both development of new organic semiconductors and new fabrication techniques. Recently, some *p*-type organic semiconductors showed comparable mobilities to amorphous silicon-based FETs.[3] However, the mobilities of the *n*-type organic semiconductors are generally less than those of the *p*-type ones, and there are a limited number of examples showing higher mobilities than 0.1 $cm^2\ V^{-1}\ s^{-1}$. The *n*-type FETs are important as key components of *p*−*n* junctions[4] and advanced electron transporting materials, where high electron mobilities and low threshold voltages are required for practical applications. To achieve a high electron mobility, the organic semiconductor has strong intermolecular interactions and a proper LUMO energy level near the work functions of the source/drain electrodes and should be highly ordered in the thin film state.[5] In early works, *n*-type organic semiconductors were prepared from electron-accepting compounds. Recently, most of them have been prepared by the introduction of electron-withdrawing groups (fluoro, perfluoroalkyl, and trifluoromethyl groups, etc.) into known *p*-type cores (naphthalene, perylene, pentacene, and oligothiophenes, etc.). Thus far, high electron mobilities have been accomplished using $F_{16}CuPC$,[6] fullerene,[7] naphthalene or perylene tetracarboxylic diimide derivatives,[8] thiophene oligomers with perfluorinated substituents,[9] quinoidal terthiophene derivatives,[10] perfluoropentacene,[11] heterocyclic oligomers with trifluoromethylphenyl groups,[12] and tetrathia-

* Corresponding author. Tel.: +81-45-924-5571; fax: +81-45-924-5489; e-mail: yoshiro@echem.titech.ac.jp.
[†] Tokyo Institute of Technology.
[‡] NHK Science and Technical Research Laboratories.

(1) (a) Forrest, S. R.; Thompson, M. E. *Chem. Rev.* **2007**, *107*, 923. (b) Yoo, B.; Jung, T.; Basu, D.; Dodabalapur, A.; Jones, B. A.; Facchetti, A.; Wasielewski, M. R.; Marks, T. J. *Appl. Phys. Lett.* **2006**, *88*, 82104. (c) Subramanian, V.; Chang, P. C.; Lee, J. B.; Molesa, S. E.; Volkman, S. K. *IEEE Trans. Compon. Packag. Technol.* **2005**, *28*, 742. (d) Baude, P. F.; Ender, D. A.; Haase, M. A.; Kelley, T. W.; Muyres, D. V.; Theiss, S. D. *Appl. Phys. Lett.* **2003**, *82*, 3964. (e) Crone, B.; Dodabalapur, A.; Lin, Y.-Y.; Filas, R. W.; Bao, Z.; LaDuca, A.; Sarpeshkar, R.; Katz, H. E.; Li, W. *Nature (London, U.K.)* **2000**, *403*, 521. (f) Gelinck, G. H.; Geuns, T. C. T.; de Leeuw, D. M. *Appl. Phys. Lett.* **2000**, *77*, 1487.
(2) Tsumura, A.; Koezuka, H.; Ando, T. *Appl. Phys. Lett.* **1986**, *49*, 1210.
(3) (a) Klauk, H.; Halik, M.; Zschieschang, U.; Schmid, G.; Radlik, W. *J. Appl. Phys.* **2002**, *92*, 5259. (b) Meng, H.; Bendikov, M.; Mitchell, G.; Helgeson, R.; Wudl, F.; Bao, Z.; Siegrist, T.; Kloc, C.; Chen, C.-H. *Adv. Mater.* **2003**, *15*, 1090. (c) Kelley, T. W.; Muyres, D. V.; Baude, P. F.; Smith, T. P.; Jones, T. D. *Mater. Res. Soc. Symp. Proc.* **2003**, *771*, 169.
(4) (a) Dimitrakopoulos, C. D.; Malenfant, P. R. L. *Adv. Mater.* **2002**, *14*, 99. (b) Sheats, J. R. *J. Mater. Res.* **2004**, *19*, 1974.
(5) Christopher, R. N.; Frisblie, C. D.; Demetrio, A.; da Dilho, S.; Bredas, J. L.; Ewbank, P. C.; Mann, K. R. *Chem. Mater.* **2004**, *16*, 4436.
(6) Bao, Z.; Lovinger, A. J.; Brown, J. *J. Am. Chem. Soc.* **1998**, *120*, 207.
(7) (a) Haddon, R. C.; Perel, A. S.; Morris, R. C.; Palstra, T. T. M.; Hebard, A. F.; Fleming, R. M. *Appl. Phys. Lett.* **1995**, *67*, 121. (b) Kobayashi, S.; Takenobu, T.; Mori, S.; Fujiwara, A.; Iwasa, Y. *Appl. Phys. Lett.* **2003**, *82*, 4581.
(8) (a) Jones, B. A.; Ahrens, M. J.; Yoon, M.-H.; Facchetti, A.; Marks, T. J.; Wasielewski, M. R. *Angew. Chem., Int. Ed.* **2004**, *43*, 6363. (b) Katz, H. E.; Lovinger, A. J.; Johnson, J.; Kloc, C.; Siegrist, T.; Li, W.; Lin, Y.-Y.; Dodabalapur, A. *Nature (London, U.K.)* **2000**, *404*, 478. (c) Malenfant, P. R. L.; Dimitrakopoulos, C. D.; Gelorme, J. D.; Kosbar, L. L.; Graham, T. O. *Appl. Phys. Lett.* **2002**, *80*, 2517.
(9) (a) Yoon, M.-H.; DiBenedetto, S. A.; Facchetti, A.; Marks, T. J. *J. Am. Chem. Soc.* **2005**, *127*, 1348. (b) Letizia, J. A.; Facchetti, A.; Stern, C. L.; Ratner, M. A.; Marks, T. J. *J. Am. Chem. Soc.* **2005**, *127*, 13476.

10.1021/cm071505s CCC: $37.00 
Published on Web 10/06/2007

**Chart 1. Chemical Structures of Thiazolothiazole Derivatives**

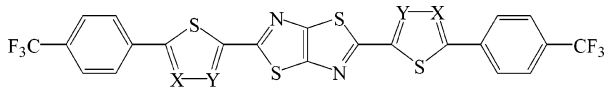

**1**: X = N, Y = CH
**2**: X = CH, Y = N
**$CF_3$-PTFZTP**: X = CH, Y = CH

fulvalene derivatives.[13] Among them, the thiazolothiazole derivative $CF_3$-PTFZTP (Chart 1 ) showed a high electron mobility of 0.3 $cm^2\ V^{-1}\ s^{-1}$ on a $SiO_2$ substrate, which was increased up to 1.20 $cm^2\ V^{-1}\ s^{-1}$ on the SCA (silane-coupling agents) treatment substrate.[14] However, this material has high threshold voltages ranging from 63 to 67 V.

In this context, we report novel semiconductors based on thiazole−thiazolothiazole $\pi$-conjugated compounds with trifluoromethylphenyl groups. These materials were designed to lower the LUMO levels by introducing electron-accepting thiazole rings, which are useful in reducing the threshold voltage of the FET device. The thiazole rings were also expected to increase the intermolecular interactions by the formation of good $\pi-\pi$-stacking as well as heteroatom contacts, which would increase the electron mobility.

## Results and Discussion

**Synthesis and Characterization.** The synthetic route to **1** and **2** is described in Scheme 1. In general, the reactivity of thiazole ring is higher at the 2-position; thus, a TMS group was used to protect the 2-position for the synthesis of **2**. The TMS group was introduced according to a literature procedure.[15] Introduction of the trifluoromethylphenyl group to the thiazole ring at each 2- and 5-position to give **1c** and **2b** was achieved by using the Negishi-coupling reaction. Formylation with *N*-formylmorpholine afforded the precursor aldehydes **1a** and **2a**. Thiazolothiazole derivatives **1** and **2** were easily synthesized in 35 and 24% yields, respectively, by a one-step reaction of the corresponding aldehydes with dithiooxamide in DMF. These materials were purified by sublimation, and the structures were characterized by the spectral data along with elemental analysis. The differential scanning calorimetry (DSC) measurement of **1** exhibited a double melting behavior at 340 and 344 °C, suggesting that

**Scheme 1. Syntheses of 1 and 2**

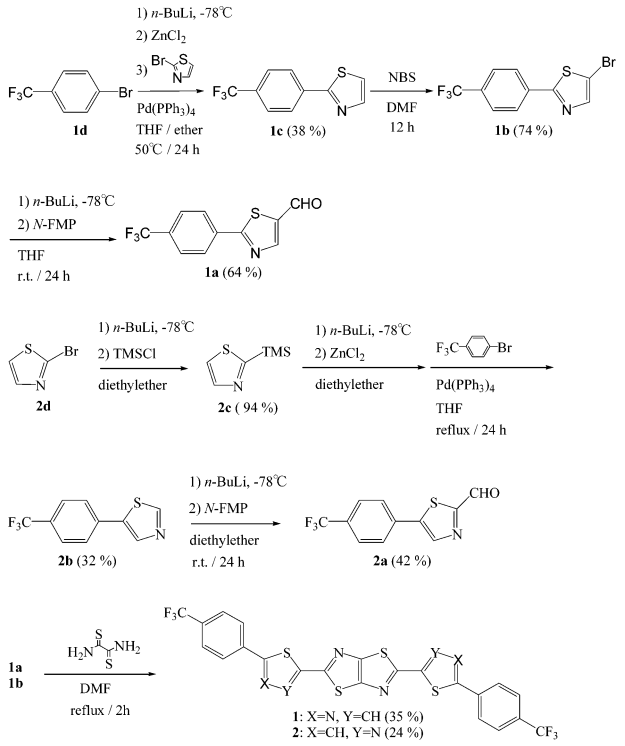


**1** has an enanthiotropic crystal polymorphism. On the other hand, **2** showed a sharp peak at 320 °C.

**Electrochemical Properties.** The reduction potentials measured by the differential pulse voltammetry (DPV) of **1** and **2** were −1.08 and −1.12 V versus SCE in dichloromethane, respectively, and their oxidation potentials were not observed. These reduction potentials are positively shifted as compared to that of $CF_3$-PTFZTP (−1.48 V vs SCE), which is attributed to the electron-accepting thiazole rings as expected. This is considered to be favorable for electron carrier injection at the semiconductor/electrode interface.

The absorption spectra of **1** and **2** in dichloromethane showed the absorption maxima at 420 and 428 nm and the end absorptions at 482 and 488 nm, respectively. The HOMO−LUMO energy gaps obtained from the end absorptions and reduction potentials were 2.57 eV for **1** and 2.54 eV for **2**. These values are larger than that of $CF_3$-PTFZTP (2.48 eV).

**X-ray Single Crystal Analysis.** Single crystals of **1** and **2** were obtained by slow sublimation. To investigate their molecular structures and intermolecular interactions in the solid states, X-ray structure analyses were carried out. Compound **1** is more planar than **2**. Thus, as shown in Figure 1, the dihedral angles between the rings in **1** are less than 5.1°, whereas those in **2** are between 5.02 and 14.59°. Their crystal structures are depicted in Figure 2. Compound **1** forms a columnar structure that is composed of three molecules in one $\pi$-stacking unit with an intermolecular distance of ca. 3.45 Å between the thiazolothiazole rings. Intermolecular S···S contacts of 3.26−3.36 Å are observed between the neighboring thiazolothiazole rings along with the *a*-axis, suggesting the presence of intercolumnar interactions. Compound **2** also forms a $\pi$-stacking structure consisting of three molecules in one unit as found in **1**. The thiazolothiazole

(10) (a) Pappenfus, T. M.; Chesterfield, R. J.; Frisbie, C. D.; Mann, K. R.; Casado, J.; Raff, J. D.; Miller, L. L. *J. Am. Chem. Soc.* **2002**, *124*, 4184. (b) Chesterfield, R. J.; Newman, C. R.; Pappenfus, T. M.; Ewbank, P. C.; Haukaas, M. H.; Mann, K. R.; Miller, L. L.; Frisbie, C. D. *Adv. Mater.* **2003**, *15*, 1278.
(11) (a) Sakamoto, Y.; Suzuki, T.; Kobayashi, M.; Gao, Y.; Inoue, Y.; Tokito, S. *Mol. Cryst. Liq. Cryst.* **2006**, *444*, 225. (b) Inoue, Y.; Sakamoto, Y.; Suzuki, T.; Kobayashi, M.; Gao, Y.; Tokito, S. *Jpn. J. Appl. Phys., Part 1* **2005**, *44*, 3663. (c) Sakamoto, Y.; Suzuki, T.; Kobayashi, M.; Gao, Y.; Fukai, Y.; Inoue, Y.; Sato, F.; Tokito, S. *J. Am. Chem. Soc.* **2004**, *126*, 8138.
(12) (a) Ando, S.; Murakami, R.; Nishida, J.; Tada, H.; Inoue, Y.; Tokito, S.; Yamashita, Y. *J. Am. Chem. Soc.* **2005**, *127*, 14996. (b) Ando, S.; Nshida, J.; Tada, H.; Inoue, Y.; Tokito, S.; Yamashita, Y. *J. Am. Chem. Soc.* **2005**, *127*, 5336. (c) Takimiya, K.; Kunigi, Y.; Ebata, H.; Otsubo, T. *Chem. Lett.* **2006**, *35*, 1200.
(13) Naraso Nshida, J.; Kumaki, D.; Tokito, S.; Yamashita, Y. *J. Am. Chem. Soc.* **2006**, *128*, 9598.
(14) Kumaki, D.; Ando, S.; Shimono, S.; Yamashita, Y.; Umeda, T.; Tokito, S. *Appl. Phys. Lett.* **2007**, *93*, 53506.
(15) Dondoni, A.; Fantin, G.; Fogagnolo, M.; Medici, A.; Pedrini, P. *J. Org. Chem.* **1988**, *53*, 1748.

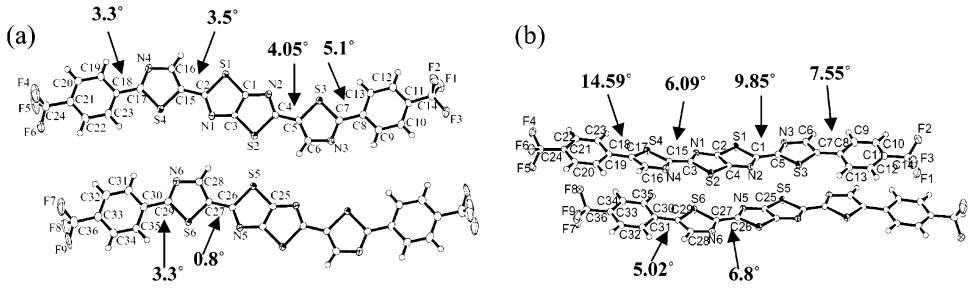


**Figure 1.** Torsion angles of (a) **1** and (b) **2**.

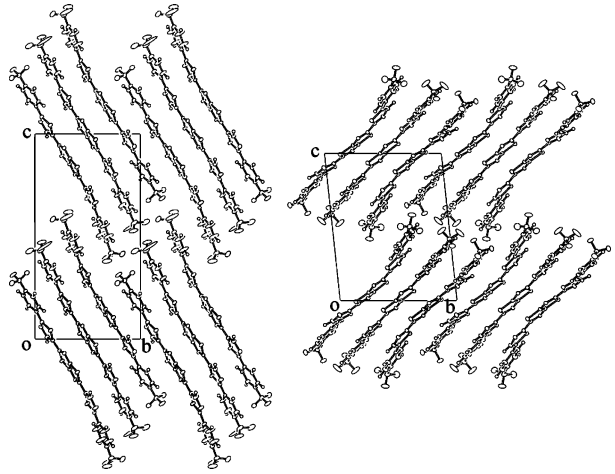


**Figure 2.** (a) Crystal structure of **1** along the *a*-axis and (b) crystal structure of **2** along the *a*-axis.

**Table 1. Field-Effect Transistor Characteristics of Bottom Contact Devices**[a]

| compound | condition | polarity | $T_{sub}$ (°C) | mobility ($cm^2\ V^{-1}\ s^{-1}$) | on/off ratio | threshold (V) |
|---|---|---|---|---|---|---|
| **1** | Bare | n | 20 | $3 \times 10^{-3}$ | $3 \times 10^4$ | 60 |
| | HMDS | n | 20 | 0.038 | $3 \times 10^6$ | 52 |
| | HMDS | n | 50 | 0.12 | $2 \times 10^7$ | 53 |
| **2** | Bare | n | 20 | | no gate effect | |
| | HMDS | n | 20 | $3 \times 10^{-4}$ | $3 \times 10^6$ | 64 |

[a] $SiO_2$: 300 nm; active layer: 50 nm; and *L*/*W*: 25 $\mu$m/294 000 $\mu$m.

rings are overlapped with the thiazole rings, and the distance between the stacked molecules is ca. 3.42 Å. The short S···S contacts of 3.55−3.65 Å between the thiazolothiazole and the thiazole rings are also observed along with the *a*-axis.

**FET Characteristics.** The FET devices were fabricated with both bottom and top contact configurations. The $SiO_2$ gate dielectric was 300 nm (bottom) or 200 nm (top) thick and was treated with hexamethyldisilazane (HMDS) or octadecyltrichlorosilane (ODTS).

The organic semiconductors were deposited at a rate of 0.2−0.3 Å/s at various substrate temperatures. In the top contact device, gold electrodes were defined after 30 nm of semiconductor deposition by using shadow masks with *W*/*L* of 1000 $\mu$m/50 $\mu$m. The FET measurements were carried out at room temperature in a high vacuum chamber ($10^{-5}$ Pa).

The FET characteristics of the bottom contact devices are summarized in Table 1. The thin film of **2** on the untreated substrate at room temperature did not show FET characteristics, whereas **1** showed a moderate electron mobility under the same condition. Although the FET of **2** on the HMDS-treated substrate behaved as an *n*-type semiconductor, the electron mobility was lower by 2 orders of magnitude as compared to the corresponding device of **1**. Although **1** and **2** have similar HOMO and LUMO energies and $\pi$-stacking structures, their FET devices showed very different behaviors. This result may be explained by the following reasons. First, **2** is more twisted, leading to the less efficient $-\pi-\pi$-overlap between the trifluoromethylphenyl groups. Second, although **1** has $\pi$-stacking between the thiazolothiazole rings, the stacking of **2** is observed between thiazolothiazole and thiazole rings and thiazole and trifluoromethylphenyl groups. Therefore, the molecules of **2** are more declined in the column, and the overlapping region is reduced. Third, the nitrogen positions affect the conjugation of the C═N double bond with the trifluoromethylphenyl group. Compound **1** has more conjugation, and the negative charge on the end group can be stabilized more.

The mobilities of **1** significantly increased depending on the deposition temperatures and surface treatment. Thus, despite the bottom contact geometry, the electron mobility became 0.12 $cm^2\ V^{-1}\ s^{-1}$ at the condition of HMDS treatment and a deposition temperature of 50 °C.

To further improve the FET performance, the devices of **1** with a top contact configuration were also fabricated. Figure 3 shows the drain/source ($I_{DS}$) current and square root of $I_{DS}$ versus gate voltage ($V_G$) characteristics at a drain voltage of 50 V for the FET devices of **1** on the $SiO_2$ substrates with or without ODTS treatment. In the transfer curves without ODTS treatment (circles in Figure 3), the rising edge of $I_{DS}$ is approximately 3 V, indicating a very low voltage drive, whereas the starting point of the on-current with ODTS treatment (triangles in Figure 3) is somewhat shifted to higher potentials. The FET characteristics of the top contact devices are summarized in Table 2. The mobilities on the bare $SiO_2$ substrate at variable temperatures were 0.24−0.26 $cm^2\ V^{-1}\ s^{-1}$, which are similar to those of $CF_3$-PTFZTP (0.12−0.30 $cm^2\ V^{-1}\ s^{-1}$). However, the threshold voltages of **1** are significantly lowered. This can be attributed to the decrease of the LUMO level. Furthermore, the ODTS-treated substrate leads to a higher mobility with a small increase in the threshold voltage. As a result, the device showed high performance *n*-type characteristics with a high electron mobility of 0.64 $cm^2\ V^{-1}\ s^{-1}$ and a relatively low threshold voltage of 24 V.

**X-ray Diffractogram.** The thin-film morphologies of **1** and **2** were examined by XRD in reflection mode (Figure 4). The reflections up to high orders were observed in all of the films, indicating the formation of lamellar ordering and

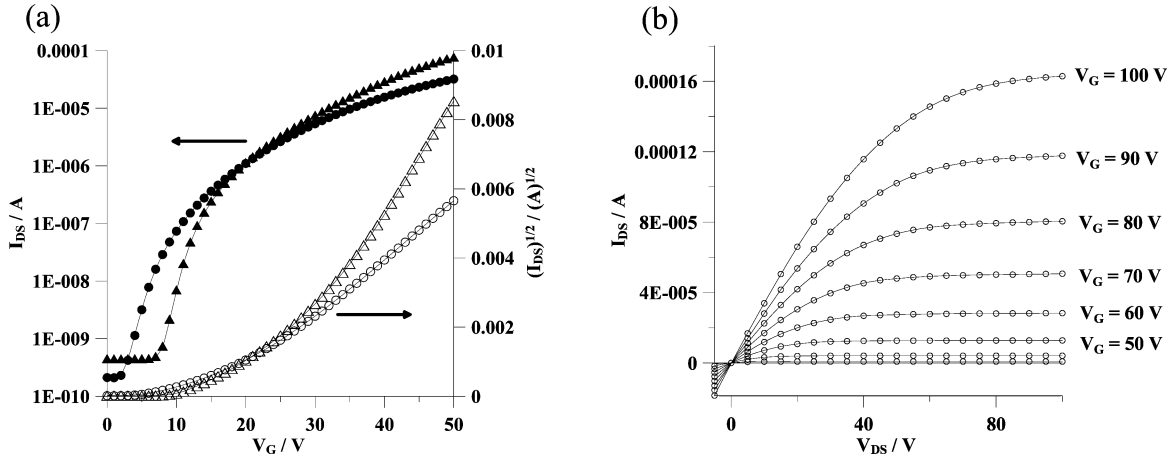


**Figure 3.** (a) Drain/source current ($I_{DS}$) and ($I_{DS}^{1/2}$) vs gate voltage ($V_G$) at a drain voltage of 50 V transfer characteristics for **1**; triangles are OFETs with ODTS treatment, and circles are OFETs with untreated substrate ($T_{sub}$ = 80 °C). (b) $I_{DS}$ vs drain/source voltage ($V_{DS}$) output characteristics for **1**; OFETs with untreated substrate ($T_{sub}$ = 80 °C).

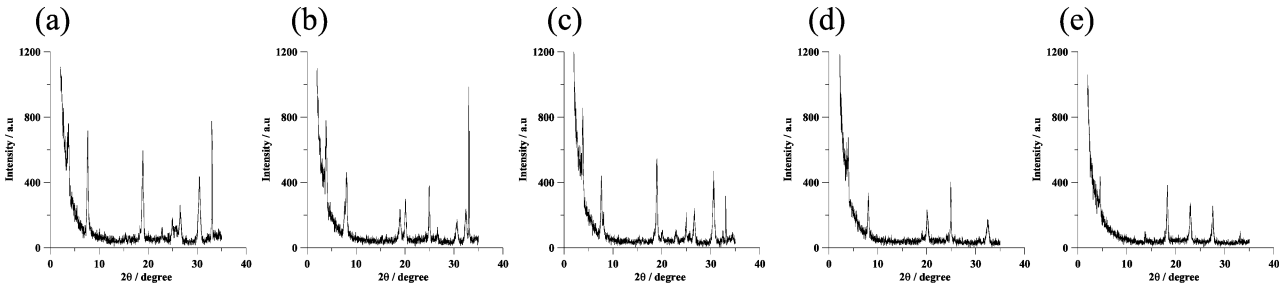


**Figure 4.** X-ray diffractograms of 50 nm films deposited on (a) untreated $SiO_2$ at room temperature for **1**, (b) HMDS-treated $SiO_2$ at room temperature for **1**, (c) untreated $SiO_2$ at 50 °C for **1**, (d) HMDS-treated $SiO_2$ at 50 °C for **1**, and (e) untreated $SiO_2$ at room temperature for **2**.

**Table 2. Field-Effect Transistor Characteristics of Top Contact Devices**[a]

| compound | condition | polarity | $T_{sub}$ (°C) | mobility ($cm^2\ V^{-1}\ s^{-1}$) | on/off ratio | threshold (V) |
|---|---|---|---|---|---|---|
| **1** | Bare | n | 20 | 0.26 | $3 \times 10^4$ | 20 |
| | Bare | n | 50 | 0.25 | $3 \times 10^4$ | 19 |
| | Bare | n | 80 | 0.24 | $2 \times 10^4$ | 18 |
| | HMDS | n | 80 | 0.38 | $3 \times 10^4$ | 28 |
| | ODTS | n | 80 | 0.64 | $7 \times 10^5$ | 24 |

[a] $SiO_2$: 200 nm; active layer: 30 nm; *L*/*W*: 50 $\mu$m/1000 $\mu$m; and *S*/*D* electrode: 50 nm Au.

crystallinity on the substrate. The *d*-spacing obtained from the first reflection peak was ca. 2.36 nm (Figure 4a), 2.28 nm (Figure 4b), 2.30 nm (Figure 4c), 2.22 nm (Figure 4d), and 1.93 nm (Figure 4e). Since the molecular lengths obtained from the single crystal X-ray analyses are 2.41 nm for **1** and 2.42 nm for **2**, the molecules are considered to have ca. 15−25° for **1** and ca. 40° for **2** declining orientations on the substrate. The molecules of **1** deposited at 50 °C on the HMDS-treated substrate have the most declined structure among them. In Figure 4b, two peaks around $2\theta = 20°$ are observed, indicating the existence of two morphologies. This finding suggests that the film of **1** takes on multi-morphologies depending on the deposition conditions. On the other hand, the films of **2** afforded the same diffractograms regardless of the deposition conditions.

## Conclusion

We have prepared two types of thiazole−thiazolothiazole derivatives with trifluoromethylphenyl groups and fabricated FET devices. The FET characteristics are strongly dependent on the nitrogen positions. The derivative with a 2-(4-trifluoromethylphenyl)thiazole unit afforded a high performance *n*-type FET device with a high mobility and low threshold voltage. The FET characteristics were related to the unique $\pi$-stacking structure and high electron affinity of the heterocyclic $\pi$-ring system.

## Experimental Procedures

**General Information.** Melting points were obtained on a Yanaco MP-500D melting point apparatus or a SHIMADZU DSC-60 instrument and are uncorrected. $^1$H NMR spectra were recorded on a JEOL JNM-ECP300 NMR spectrometer, and chemical shifts were referenced to tetramethylsilane (TMS). Elemental analyses were carried out with a LECO/CHNS-932 analyzer (Chemical Resources Laboratory at the Tokyo Institute of Technology). EI mass spectra were collected on a JEOL JMS-700 mass spectrometer. UV−vis spectra were recorded on a SHIMADZU Multi Spec-1500 spectrometer. Emission spectra were collected on a JASCO FP-6600 spectrometer. Differential pulse voltammograms were recorded on a BAS-100B system containing tetrabutylammonium hexafluorophoshate ($TBAPF_6$) (0.1 mol $dm^{-3}$ in dry dichloromethane). The Pt disk, Pt wire, and SCE were used as the working, counter, and reference electrodes, respectively. Elemental analyses were performed at the Tokyo Institute of Technology, Chemical Resources Laboratory.

**X-ray Analysis.** The measurements were carried out on a Rigaku RAXIS-RAPID Imaging Plate diffractometer (Mo− Kα radiation, $\lambda = 0.71075$ Å). The data were collected at 93 K, and the structures were solved by the direct method (SIR97) and expanded using Fourier techniques. Non-hydrogen atoms were refined anisotropi-

cally. Hydrogen atoms were placed in geometrically calculated positions.

**Crystal Data for 1.** $C_{24}H_{10}N_4S_4F_6$, $M = 596.60$, crystal dimensions 0.70 mm × 0.07 mm × 0.03 mm, triclinic, space group $P\bar{1}$, $a = 5.914(10)$ Å, $b = 12.19(2)$ Å, $c = 23.72(3)$ Å, $\alpha = 89.06(6)$, $\beta = 97.98(7)$, $\gamma = 97.16(7)$, $V = 1679(15)$ Å$^3$, $Z = 3$, $D_c = 1.769$ g cm$^{-3}$, 16 361 reflections collected, 7638 independent ($R_{int} = 0.053$), GOF = 0.87, $R_1 = 0.053$, $wR_2 = 0.108$ for all reflections. The CCDC reference number is 648764.

**Crystal Data for 2.** $C_{24}H_{10}N_4S_4F_6$, $M = 596.60$, crystal dimensions 0.70 mm × 0.10 mm × 0.01 mm, triclinic, space group $P\bar{1}$, $a = 8.43(1)$ Å, $b = 13.05(2)$ Å, $c = 16.35(3)$ Å, $\alpha = 93.22(6)$, $\beta = 101.18(5)$, $\gamma = 103.56(5)$, $V = 1705(15)$ Å$^3$, $Z = 3$, $D_c = 1.742$ g cm$^{-3}$, 16 351 reflections collected, 7563 independent ($R_{int} = 0.032$), GOF = 0.99, $R_1 = 0.042$, $wR_2 = 0.084$ for all reflections. The CCDC reference number is 648765.

**Fabrication of OFETs. Bottom Contact Devices.** OFETs were constructed on heavily doped *n*-type silicon wafers covered with 300 nm thick thermally grown silicon dioxide. The silicon dioxide acts as a gate dielectric layer, and the silicon wafer serves as a gate electrode. Cr (10 nm)/Au (20 nm) was successively evaporated and photolithographically delineated to obtain the source and drain electrodes. The channel width ($W$) and length ($L$) were 294 000 and 50 $\mu$m, respectively. Organic compounds were deposited on the channel regions by vacuum evaporation at a rate of 0.2−0.3 Å s$^{-1}$ under a pressure of $10^{-5}$ Pa. The thickness of the semiconductor layer was 500 Å. The FET measurements were carried out at room temperature in a vacuum chamber ($10^{-5}$ Pa). The output and transfer characteristics of **1** and **2** by bottom contact configuration are shown in Figures S3−S6 in the Supporting Information.

**Top Contact Devices.** OFETs were constructed on heavily doped *n*-type silicon wafers covered with 200 nm thick thermally grown silicon dioxide. The silicon dioxide acts as a gate dielectric layer, and the silicon wafer serves as a gate electrode. Organic compounds were deposited on the silicon dioxide by vacuum evaporation at a rate of 0.1−0.3 Å s$^{-1}$ under a pressure of $10^{-5}$ Pa. The thickness of the semiconductor layer was 300 Å. During the evaporation, the temperature of the substrate was maintained by heating a copper block on which the substrate was mounted. Gold was used as the source/drain electrode and was deposited on the organic semiconductor layer through a shadow mask with a channel width ($W$) of 1000 $\mu$m and a channel length ($L$) of 50 $\mu$m. Finally, the FET measurements were carried out at room temperature in the vacuum chamber ($10^{-5}$ Pa) without exposure to air with Hewlett-Packard 4140A and 4140B models.

**Materials.** 4-Bromobenzotrifluoride and 2-bromothiazole were purchased from Tokyo Kasei Co. and used without further purification. Tetrakis(triphenylphosphine)palladium(0), *n*-butyllithium in *n*-hexane, zinc chloride, and THF were purchased from Kanto Chemicals and used without further purification. Dithiooxamide was purchased from Wako Co. and used without further purification.

**Synthesis. 5-Bromo-2-(4-trifluoromethylphenyl)thiazole (1b).** *N*-Bromosuccinicimide (2.76 g, 15.5 mmol) was added to a solution of 2-(4-trifluoromethylphenyl)thiazole (**1c**) (3.52 g, 15.4 mmol) in DMF (50 mL). The solution was stirred for 12 h at 60 °C. Water was added, and the solution was filtered. The residue was purified by column chromatography (silica gel, 1:1 hexane/dichloromethane) to give **1b** (3.52 g, 74%) as a pale yellow solid. $^1$H NMR $\delta$/ppm = 7.99 (d, 2H, $J = 8.4$ Hz); 7.80 (s, 1H); 7.71 (d, 2H, $J = 8.4$ Hz).

**2-(4-Trifluoromethylphenyl)thiazole-5-carbaldehyde (1a).** To a solution of 5-bromo-2-(4-trifluoromethylphenyl)thiazole (**1b**) (3.52 g, 11.4 mmol) in THF (80 mL) was added *n*-BuLi (1.59 M solution in *n*-hexane, 8.5 mL, 13.5 mmol) at −78 °C. After stirring for 1 h, a solution of *N*-formylmorpholine (1.35 g, 11.7 mmol) in THF (20 mL) was added. After additional stirring for 1 h at −78 °C, the mixture was allowed to warm to room temperature and then was hydrolyzed with 1 N HCl. The aqueous phase was extracted with dichloromethane. The organic layer was dried over $Na_2SO_4$, and the solvent was evaporated. The remaining solid was purified by column chromatography on silica gel to give **2a** (1.89 g, 64%) as a yellow solid. $^1$H NMR $\delta$/ppm = 10.1 (s, 1H); 8.49 (s, 1H); 8.16 (d, 2H, $J = 8.4$ Hz); 7.76 (d, 2H, $J = 8.4$ Hz).

**5-(4-Trifluoromethylphenyl)thiazole (2b).** A solution of 2-(trimethylsilyl)thiazole (**2c**) (4.46 g, 28.2 mmol) in diethyl ether (30 mL) was added over 30 min to a stirred solution of *n*-BuLi (1.58 M solution in *n*-hexane, 19.5 mL, 30.8 mmol) in the same solvent (50 mL) at −78 °C. After stirring the reaction mixture for 1 h, a solution of $ZnCl_2$ (3.88 g, 28.5 mmol) in diethyl ether (20 mL) was added. After 1 h at −78 °C, the reaction mixture was allowed to warm to room temperature to which were added 4-bromobenzotrifluoride (6.38 g, 28.3 mmol) in THF (100 mL) and tetrakis(triphenylphosphine)palladium(0) (0.207 g). The mixture was refluxed for 24 h. After cooling to room temperature, the solvent was removed under vacuum, and the crude mixture was treated with 1 N HCl and extracted with dichloromethane. The organic layer was dried over anhydrous $Na_2SO_4$, and the solvent was removed in vacuo. Column chromatography of the residue (silica gel, dichloromethane) gave 2.03 g (32%) of **2b** as a yellow solid. $^1$H NMR $\delta$/ppm = 8.84 (s, 1H); 8.17 (s, 1H); 7.69 (m, 4H).

**5-(4-Trifluoromethylphenyl)thiazole-2-carbaldehyde (2a).** To a solution of 5-(4-trifluoromethylphenyl)thiazole (**2b**) (1.77 g, 7.72 mmol) in diethyl ether (150 mL) was added *n*-BuLi (1.57 M solution in *n*-hexane, 5.0 mL, 7.85 mmol) in the same solvent (30 mL) at −78 °C. After stirring for 2 h, a solution of *N*-formylmorpholine (0.889 g, 7.72 mmol) in diethyl ether (30 mL) was added. After additional stirring for 1 h at −78 °C, the mixture was allowed to warm to room temperature and then hydrolyzed with 1 N HCl. The aqueous phase was extracted with dichloromethane. The organic layer was dried over $Na_2SO_4$, and the solvent was evaporated. The remaining solid was purified by column chromatography on silica gel to give **2a** (0.824 g, 42%) as a yellow solid. $^1$H NMR $\delta$/ppm = 9.99 (s, 1H); 8.33 (s, 1H); 7.75 (m, 4H).

**2,5-Bis[2-(4-trifluoromethylphenyl)thiazol-5-yl]thiazolo[5,4-*d*]thiazole (1).** A solution of dithiooxamide (0.271 g, 2.25 mmol) and 2-(4-trifluoromethylphenyl)thiazole-5-carbaldehyde (**1a**, 0.934 g, 3.63 mmol) in DMF (25 mL) was refluxed for 2 h. The mixture was cooled to room temperature, and water was added. Then, the solution was filtered. The yellow residue was purified by sublimation to give **1** (0.381 g, 35.2%) as pale orange crystals. Mp 342−345 °C. MS/EI (70 eV) : $m/z$ 596($M^+$, 100%), 577(4.8%, M − F), 425(3.8%, M − $CF_3PhCN$), 298(4.3%, M − $C_{12}H_5F_3N_2S_2$), 254($C_{10}H_5F_3NS$ − $CN^{+\cdot}$). Anal. calcd for $C_{20}H_{10}N_2S_4$: C, 48.32; H, 1.69; N, 9.39; S, 21.50. Found: C, 48.34; H, 1.88; N, 9.20; S, 21.51.

**2,5-Bis[5-(4-trifluoromethylphenyl)thiazol-2-yl]thiazolo[5,4-*d*]thiazole (2).** A solution of dithiooxamide (0.204 g, 1.70 mmol) and 5-(4-trifluoromethylphenyl)thiazole-2-carbaldehyde (**2a**, 0.824 g, 3.21 mmol) in DMF (15 mL) was refluxed for 2 h. The mixture was cooled to room temperature, and water was added. Then, the solution was filtered. The yellow residue was purified by sublimation to give **2** (0.233 g, 24.4%) as pale orange crystals. Mp 319−322 °C. MS/EI (70 eV) : $m/z$ 596($M^+$, 100%), 577(4.6%, M − F), 298(8.8%, M − $C_{12}H_5F_3N_2S_2$), 202(25.8%, M − $CF_3PhTzFZCN$). Anal. calcd for $C_{20}H_{10}N_2S_4$: C, 48.32; H, 1.69; N, 9.39; S, 21.50. Found: C, 48.43; H, 1.99; N, 9.37; S, 21.79.

**Acknowledgment.** This work was supported by a Grant-in-Aid for Scientific Research on Priority Areas (15073212) from the Ministry of Education, Culture, Sports, Science and

Technology, Japan and the Mizuho Foundation for the Promotion of Sciences.

**Supporting Information Available:** Differential pulse voltammograms, UV−vis absorption spectra, FET characteristics of bottom contact devices, XRD pattern, and X-ray crystallographic information files (CIF). This material is available free of charge via the Internet at http://pubs.acs.org.

CM071505S